Journal of Chromatography A 1783 (2026) 467145

Contents lists available at ScienceDirect

Journal of Chromatography A

journal homepage: www.elsevier.com/locate/chroma

Addressing method transfer and robustness challenges using design space modeling

Arnold Zöldhegyi [a,b], Krisztián Horváth [a], Imre Molnár [b], Róbert Kormány [c,*]

[a] Analytical Chemistry Research Group, University of Pannonia, Egyetem u. 10, 8200 Veszprém, Hungary
[b] Molnár-Institute for Applied Chromatography, Schneeglöckchenstrasse 47, 10407 Berlin, Germany
[c] Egis Pharmaceuticals Plc., Keresztúri út 30-38, Budapest, Hungary

ARTICLE INFO

Keywords:
Instrument-to-instrument differences
Method transfer and robustness challenges
Compensation strategies
Design space analysis and comparison

ABSTRACT

In high-performance liquid chromatography (HPLC), robust and easily transferable analytical methods are essential to ensure consistent performance throughout the entire lifecycle of an analytical procedure, including unforeseen future applications. Nevertheless, robustness-, and ruggedness-related issues are frequently reported in industrial practice, particularly during method transfer between laboratories. These challenges often arise from incomplete method understanding and insufficient consideration of HPLC system-related effects, such as dwell volume, extra-column contributions and other, at first less evident, instrument-to-instrument variations in solvent delivery, mixing behavior and column thermal control.

In this context, modeling approaches aligned with Analytical Quality by Design (AQbD) principles provide valuable support for both proactive method development and reactive troubleshooting. In the current work, we used DryLab modeling Design Spaces (DSs) to create digitized modeling fingerprints of various instruments, enabling extensive in silico investigations, including in-depth assessment of method transferability and evaluation of subtle, instrument-dependent robustness characteristics.

1. Introduction

Liquid chromatography (LC) is one of the most widely used analytical techniques in pharmaceutical, biopharmaceutical, food, and environmental analysis. As analytical procedures are routinely applied across multiple laboratories throughout their lifecycle, they must deliver consistent performance. This is commonly referred to as analytical procedure robustness or when intra-laboratory variations are considered, such as the case of working across various instruments, intermediate precision (ruggedness). Accordingly, robustness and intermediate precision have become a central focus of current regulatory guidelines, where systematic understanding facilitates risk mitigation associated with future changes. While ICH Q2(R2) and ICH Q14 address hardware-related parameters (e.g., column lot, detection wavelength) and applied method conditions (e.g., mobile phase composition, pH, column temperature, flow rate), potential differences between HPLC instruments themselves are not explicitly considered. Meanwhile, the recent update of USP–NF <621> highlights backpressure as a factor that may influence chromatographic behavior [1–3].

Since its early development by Csaba Horváth in the 1960s, HPLC technology has evolved from "high-pressure" liquid chromatography to high-performance liquid chromatography (HPLC) and more recently ultra-high-performance liquid chromatography (UHPLC). Today, numerous vendors offer distinct platforms with differing hardware designs and technological solutions [4,5]. As methods are routinely transferred across such systems, instrument-to-instrument variability has become an increasingly relevant factor in ensuring robust and transferable chromatography. This is particularly critical for gradient methods, which are more susceptible to transfer-related challenges than isocratic separations [6–8].

At first glance, all HPLC instruments share the same fundamental components: mobile-phase reservoirs (typically equipped with a degasser), a solvent delivery system, a sample introduction device (injector), a chromatographic column, a detector, a data acquisition system, and the associated tubing and fittings. As illustrated in Fig. 1, however, these components may differ substantially in both design and performance, potentially leading to significant differences in retention times, selectivity and observed peak-widths. For example, most HPLC systems employ constant-flow pumps based on twin-head reciprocating piston mechanisms. In contrast, Waters UPLC systems introduced an

* Corresponding author.
E-mail address: kormany.robert@egis.hu (R. Kormány).

https://doi.org/10.1016/j.chroma.2026.467145
Received 23 March 2026; Received in revised form 26 May 2026; Accepted 27 May 2026
Available online 28 May 2026
0021-9673/© 2026 Elsevier B.V. All rights are reserved, including those for text and data mining, AI training, and similar technologies.

alternative design in 2004 utilizing a primary- and an accumulator pump-driven solvent delivery system, engineered to minimize flow pulsation and automatically compensate for mobile-phase compressibility. Solvent compressibility becomes increasingly relevant at elevated pressures (up to 15,000 psi), whereas other systems rely on predefined or user-adjustable compressibility settings. Since all pump designs incorporate moving mechanical components subject to wear, solvent delivery performance may vary over time even between nominally identical instruments, necessitating regular maintenance and recalibration [9,10].

In addition to pump design, solvent-mixing solutions used to generate gradient programs represent another major source of system variability. These are generally classified as low-pressure gradient (LP) and high-pressure gradient (HP) systems. In LP systems—typically employing electronically controlled proportioning or solenoid valves—solvent mixing occurs upstream of the pump heads and is usually accompanied by larger dwell volumes compared to HP systems. A characteristic feature of this design is that any deviation in proportioning valve performance may directly affect gradient composition; therefore, routine verification of solvent channel accuracy is recommended. In contrast, HP systems use dedicated pumps to pressurize individual solvents prior to mixing. HP-mixing generally provides superior gradient accuracy and reproducibility, particularly at low flow rates and elevated pressures. As both LP and HP systems are commonly encountered in analytical laboratories, careful consideration is needed when transferring established gradient methods between different instrument types. In addition, solvent mixers may also vary across platforms, with some systems incorporating passive mixing chambers and others employing proprietary microfluidic mixing technologies [9,11,12].

In this context, the volume of the fluidic path extending from the point of solvent mixing to the head of the chromatographic column can differ substantially between various instruments. This volume—commonly referred to as the dwell volume (V_D) or gradient delay volume—is particularly relevant for gradient separations, as it directly affects gradient timing at the column inlet. Consequently, differences in V_D must be experimentally determined and known during gradient method transfer from one instrument to another. A common and practical approach to minimizing its effect is to modify the gradient program by introducing an additional initial isocratic hold before the gradient program, thereby matching the effective V_D to that of the system with the largest V_D. When transferring methods between systems, adjusting the duration of this initial isocratic segment allows V_D differences to be readily compensated. An alternative strategy is to delay sample injection relative to the start of the gradient; however, this approach requires highly precise timing and is therefore less commonly applied in routine practice. Some vendors also offer proprietary software to emulate another instrument (including HP–LP transferability) possessing a higher V_D, to alleviate some of these challenges [13–16].

Another well-known instrument-specific volume contribution is the extra-column volume (V_{ECV}), which arises from the hydrodynamic nature of HPLC systems. As a small injected sample volume travels through the connecting capillaries, detector flow cell (and the column itself), band broadening occurs due to differences in linear velocity between the fluid at the center of the tubing and that near the walls. This hydrodynamic dispersion contributes to peak broadening outside the chromatographic column. A commonly accepted rule is that extra-column effects—typically expressed as variance (σ^2)—should contribute no more than approximately 10% of the total band broadening generated within the stationary phase. Exceeding this limit can significantly compromise separation efficiency, particularly for high-efficiency or short columns. As a result, preserving intrinsic column efficiency becomes more challenging with narrow-bore (2.1 mm) columns, which are typically used with UHPLC systems designed to minimize V_{ECV}. An additional, often overlooked source of apparent band broadening might arise from signal digitization and detector data processing. The sampling rate itself does not broaden a chromatographic band if the signal is sampled instantaneously. However, if each recorded point represents an average over the acquisition interval Δt, the operation is equivalent to boxcar averaging and adds a variance contribution of $\Delta t^2/12$ to the observed peak variance. Since manufacturers do not always document whether data points are instantaneous, averaged, or additionally filtered, this effect should be verified experimentally by recording the same peak at different sampling rates and checking whether the measured variance increases approximately with Δt^2. Such data-acquisition effects can lead to an apparent digital loss of resolution, particularly for narrow UHPLC peaks [6,9,17,18].

Various experimental protocols for determining both V_D and V_{ECV} have been described in the literature and are comprehensively reviewed by several authors [9,11]. Of particular importance, when changing column dimensions (length, diameter, particle size) or mobile phase flow rate, the ratio between V_D and the liquid volume of the column (*dead or hold-up volume*, V_0) must also be maintained constant. Keeping the original ratio ensures the formation of comparable intrinsic gradient profiles within the geometrically scaled systems. Currently, most major column manufacturers provide geometrical method transfer calculators that facilitate reliable up- or downscaling between HPLC and UHPLC conditions. These tools typically account for column geometry, injected sample volume, gradient program parameters, and system-related volumes such as V_D and V_{ECV}. However, their functionality is generally limited to a one-step vertical transfer of predefined operating conditions

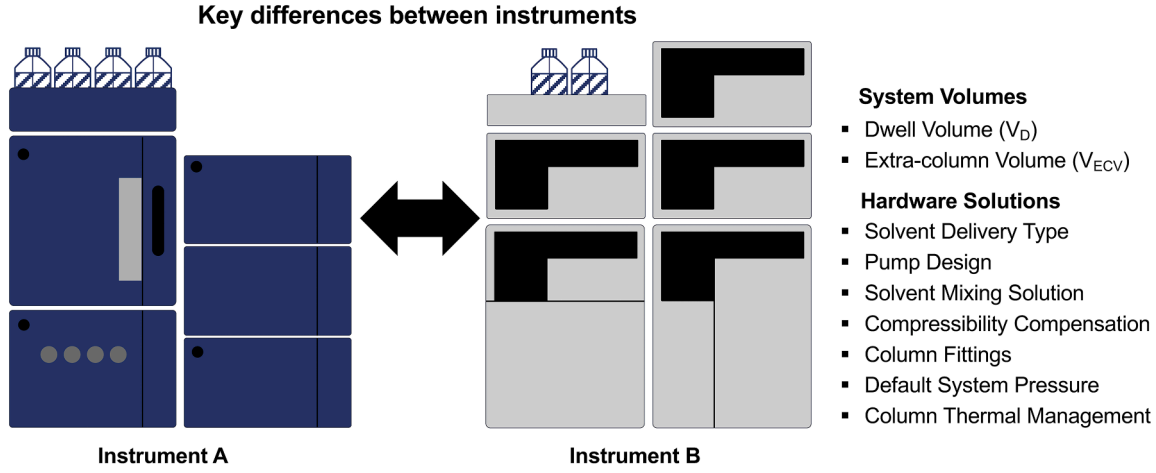


Fig. 1. Schematic overview of system-to-system differences. Although system volume differences are well known and can relatively easily be accounted for; however, various hardware solutions may further complicate method transfer across UHPLC and HPLC systems.

and does not extend to a broader, systematic evaluation of method robustness or multidimensional parameter interdependencies. Another potential source of method transferability issues may originate from the core of the separation process: the chromatographic column itself. Although batch-to-batch variations within a given stationary phase are typically minor, they are nevertheless unavoidable. More importantly, competitive stationary phases sourced from different manufacturers sharing very similar or identical physicochemical properties in terms of particle size-, packing chemistry and morphology may also exhibit substantially different selectivity profiles [14,16,19,20].

Furthermore, precise and reproducible column temperature control is a fundamental component of any RPLC method specification, as analyte retention can generally be expressed by the Gibbs free energy or the van't Hoff equation. In its linearized form, this relationship assumes a linear dependence between the logarithm of the retention factor and the reciprocal absolute temperature (1/T), assuming that the enthalpy (ΔH°) and entropy (ΔS°) terms remain temperature-independent over the investigated range. Values of the retention factor (k) usually decrease with increasing temperature by 1–2% per°C [21,22]. This thermodynamic framework has been widely validated for small molecules and, within moderate temperature intervals, also for larger molecules across various chromatographic modes. Nevertheless, when broader temperature ranges are explored, or in case of some ortho-, meta-, and para-substituted drug analogues, a more pronounced non-linear relationship might be observed, suggesting complex temperature-dependent changes in the underlying retention mechanisms [23–25]. These examples illustrate that precise thermal management of the chromatographic column is of utmost importance for adjusting and controlling peak-retentions. It is therefore somewhat surprising that certain compendial methods still do not explicitly mandate controlled column temperature conditions, thereby potentially compromising method robustness and transferability [26].

Conventional instrument column ovens typically allow temperature regulation within a range extending from approximately 10°C below ambient temperature up to 60–70°C, depending on the instrument configuration and cooling capacity. From a technical perspective, most column ovens are equipped with either a simple block heater or a more advanced Peltier-based temperature control unit equipped with a thermocouple capable of both heating and cooling, positioned adjacent to the column. This configuration is frequently supplemented by a preheater unit to thermally equilibrate the mobile phase prior to entering the column, thereby minimizing temperature mismatch effects. However, the additional tubing associated with such preheaters increases the system V_D and V_{ECV}. An alternative thermal management approach involves still-air column compartments or, more commonly, forced-air circulation systems. These designs rely primarily on convective rather than conductive heat transfer, and since air is a less efficient conductor of heat than metal, column temperature equilibration may require longer stabilization times compared with block-type heaters [10,11]. Because both the mobile phase within the column and the packing along with the stainless-steel column housing represent substantial thermal masses, each oven design can exhibit distinct characteristics with respect to achieved temperature homogeneity, thermal response time, and overall heat transfer efficiency [27–29].

Indeed, according to Darcy's law, forcing a liquid through a packed stationary phase generates a substantial pressure differential between the column inlet and outlet, commonly referred to as column backpressure. This backpressure is directly proportional to the viscosity of the mobile phase and the averaged mobile-phase velocity and inversely proportional to the square of the particle diameter of the packing material. As a result, modern UHPLC systems packed with sub-2 μm particles routinely operate at pressures approaching 15,000 psi (≈1000 bar). Under such conditions, as the pressurized liquid traverses the porous packing bed, a substantial amount of mechanical energy is imparted to the mobile phase by the pump and irreversibly dissipated through viscous friction, resulting in significant heat generation within the column. This phenomenon, commonly termed frictional heating, can be resolved into axial and radial components—a subject that attracted considerable attention already during the early development of HPLC [17,30,31].

The axial temperature gradient develops along the column length as a consequence of the progressive pressure decrease from inlet to outlet, potentially inducing spatial variations in the analyte-stationary phase equilibrium and, consequently, in the retention factor. In contrast, the radial temperature gradient arises from the interplay between internal heat generation and limited heat dissipation through the column wall. This radial temperature non-uniformity is primarily responsible for efficiency loss, as temperature-dependent variations in mobile-phase viscosity across the column cross-section impair mass-transfer and promote band broadening.

Because radial heat transfer is inherently restricted—particularly in columns with larger internal diameters (e.g., 4.6 mm)—heterogeneous temperature profiles may develop, further contributing to peak dispersion. This consideration largely explains the widespread adoption of narrow-bore (2.1 mm) column formats in UHPLC applications, which more effectively mitigate radial frictional heating effects. Bearing this in mind, significant differences in axial and radial thermal profiles can be expected depending on the applied thermostatting mode [32,33].

Beyond these considerations, it is also true that different chromatographic instruments may exhibit distinct default system backpressures, mainly determined by the total length and internal diameter of the connecting capillaries. These capillaries are often color-coded and available in various internal diameters as kits to accommodate specific pressure and volume requirements. Variations in capillary dimensions between instruments can therefore influence both system pressure characteristics and extra-column dispersion.

At last, it is also important to emphasize that instruments may differ in additional design features which, particularly in the context of modern large-molecule analyses such as monoclonal antibodies and oligonucleotides, can significantly influence non-specific adsorption of the analytes. Such interactions may lead to substantially reduced peak efficiency, manifested as substantial band broadening and tailing, as well as recovery losses. For this reason, instrument vendors have devoted considerable effort to developing highly inert HPLC-systems, incorporating alternative construction materials such as titanium or proprietary organosiloxane-coating, in addition to conventional materials including stainless steel, polytetrafluoroethylene (PTFE) and polyether ether ketone (PEEK) polymer [10,11,34].

In a precursor study, supported by *in silico* modeling, we demonstrated a successful transfer of a developed gradient method across different column formats (length, internal diameter, and particle size) with identical stationary phase chemistry, as well as across various UHPLC and HPLC systems, for loratadine and its European Pharmacopoeia (Ph. Eur.)-specified impurities [35]. Since then, our group has further developed an analytical Design Space (DS) modeling approach to explore both similarities and differences in selectivity among various USP L1-type stationary phases [36]. This methodology was also applied to evaluate batch-to-batch reproducibility of an ethylene-bridged hybrid stationary phase[20], to investigate differences between two elution modes in cation-exchange (CEX) separations of monoclonal antibodies [37], to enable rapid comparisons of column chemistries[38], and more recently, to compare volatile and non-volatile buffer systems under identical nominal pH conditions [39]. Taken together, these studies highlighted the need for systematic, analytical Quality-by-Design (AQbD) oriented approaches to unravel the complex interplay between stationary phase properties, applied method conditions, and analyte characteristics. The resulting modeling "fingerprints" proved to be highly sensitive and provided deeper insight than traditional characterization and comparison methods.

On this theoretical basis, we revisited the topic of method transfer, focusing specifically on instrument-to-instrument transferability supported by DS modeling, with the aim of moving beyond the conventional

concept of simple vertical transfer based solely on compensated system volumes (V_D, V_{ECV}), as typically applied in routine practice. European Pharmacopoeia (Ph. Eur.)-specified impurities were selected as model analytes due to their pharmaceutical relevance and demonstrated suitability in similar studies. The primary objective was therefore to assess method transferability across instruments possessing somewhat different technological designs using an established two-dimensional (t_G–T) DryLab modeling and subsequent comparative workflow.

2. Materials and methods/experimental part

2.1. Chemicals

2.1.1. Limited geometrical scaling study

Test substances (thiourea, 2-methylbenzylamine, pyridine, 2,6-lutidine, 2-picoline, 2,4-lutidine, 3-picoline, aniline, benzyl alcohol, 3,4-lutidine) for the limited geometrical scaling experiments were purchased from Merck (Darmstadt, Germany). Eluent composition was acetonitrile–0.025 M potassium phosphate adjusted to pH 5.8 (15:85, v/v). The solution was freshly prepared and filtered before use through a regenerated cellulose filter membrane with a 0.2 μm pore size (Sartorius, Goettingen, Germany). The organic mobile phase (eluent B) was acetonitrile (ACN) and was purchased from Merck (Darmstadt, Germany).

2.1.2. Systematic modeling analysis

Reference standards—amlodipine and Ph. Eur.-impurities A, B, D, E, F, G, and H—were obtained from Egis Pharmaceuticals Plc. (Budapest, Hungary). The sample solvent consisted of acetonitrile/water (30/70, v/v).

Throughout the model analyses, the aqueous mobile phase (eluent A) comprised 0.1% (v/v) perchloric acid in water. The pH of a 0.1% $HClO_4$ solution is about 2.0, which effectively suppresses the ionization of the acidic impurity (Imp H) and minimizes residual silanol activity on the silica-based stationary phase. Furthermore, as earlier proven, under these acidic conditions, the high concentration of hydronium ions (H_3O^+) ensures stable ionic properties of the mobile phase [39].

2.2. Equipment, software

Limited geometrical scaling experiments were performed on a Waters Acquity Classic UPLC system, with the temperature set to 30°C. The restriction unit was a 10 cm × 25 μm I.D. capillary, purchased from IDEX Health Science (Northbrook, Illinois, USA) contributing only a negligible V_{ECV} addition of approximately 50 nL.

Modeling experiments were conducted on 4 different UHPLC and UPLC systems (UPLC is a registered brand of Waters):

1. Waters Acquity Classic UPLC system equipped with a high-pressure binary solvent delivery pump, an autosampler, and a photodiode array detector. The chromatographic system had a 5 μL injection loop and a 500 nL flow cell, with a measured V_D of 100 μL.
2. Waters Acquity H-Class UPLC system equipped with a low-pressure quaternary solvent delivery pump, a flow-through needle injector (FTN), and a photodiode array detector with a measured V_D of 380 μL.
3. Agilent Infinity 1290 UHPLC system equipped with a low-pressure quaternary solvent delivery pump, a flow-through needle injector (FTN), and a photodiode array detector with a measured V_D of 500 μL.
4. Shimadzu Nexera X2 UHPLC system equipped with a high-pressure binary solvent delivery pump, a flow-through needle injector (FTN), and a photodiode array detector with a measured V_D of 200 μL.

It should be noted that the V_{ECV} used in the gradient models was treated as an effective post-column contribution rather than as an experimentally measured total system V_{ECV}. Conventional V_{ECV} measurements are typically performed under isocratic conditions and include both pre-column and post-column contributions. In gradient separations, however, these two contributions are not equivalent. Pre-column sample dispersion may be substantially mitigated by on-column band focusing under sufficiently retentive initial conditions, while the influence of the pre-column fluidic path on gradient timing is primarily reflected in the V_D, which was experimentally determined and compensated where required. In contrast, the post-column volume, including connecting tubing and the detector flow cell, may contribute to both a small retention shift and additional peak broadening. At the applied flow rate of 0.5 mL/min, even a post-column volume of 10 μL would correspond to a retention shift of only 0.020 min. If this residence interval is approximated as a rectangular averaging window, the additional temporal variance is $\Delta t^2/12$, corresponding to 1.3×10^{-6}–3.3×10^{-5} min^2 for post-column volumes between 2 and 10 μL. This contribution is small relative to the chromatographic effects discussed in this work and is not expected to affect the location or stability of the DS boundaries. Therefore, effective post-column V_{ECV} values of 4–5 μL were used in the gradient models, which provided good agreement with the calibrated modeling peak widths.

For the two Waters systems, instrument control and data acquisition were managed using Empower CDS ver. 3.8 (Waters, Milford, USA), whereas the Agilent system was controlled with OpenLab ver. 2.8 (Santa Clara, California, USA), and the Shimadzu system with LabSolutions ver. 5.8 (Kyoto, Japan). Chromatographic processing for the limited geometrical scaling experiments and DS experiments was performed at 200 and 237 nm, respectively.

DS models, robustness and DS comparison studies were developed using DryLab 4 (ver. 4.6) modeling software package (Molnár-Institute, Berlin, Germany). pH measurements were performed using an MP 225 pH-meter (Mettler-Toledo, Greifensee, Switzerland).

2.3. Stationary phase selection

For the limited geometrical scaling experiments, a bridged ethylene-hybrid type BEH C18 UPLC and corresponding XBridge C18 HPLC chemistries were used in three different formats: 50 × 2.1 mm (1.7 and 5 μm) and 100 × 2.1 mm (1.7 μm).

Further DS modeling analyses were performed on Waters Acquity BEH C18 columns in two formats: 50 × 2.1 and 100 × 2.1 mm, both packed with 1.7 μm fully porous particles. To create a common platform and avoid potential minor batch-to-batch variations we used the same stationary phases throughout all experiments on the tested UHPLC systems.

3. Theory and calculations

3.1. Pressure effects—reevaluating earlier results

Pressure effects formed the conceptual basis of the present investigation. Pressure-induced changes in retention are commonly explained by variations in the partial molar volume of the solute (ΔV_m). In particular, for large molecular species, increasing pressure may enhance solute adsorption and thereby alter retention behavior. This phenomenon has been systematically studied, and its potential for revealing novel selectivities—especially for biomolecules such as oligopeptides and monoclonal antibodies, both at intact and subunit levels—has been highlighted in a recent work [40].

In a preceding base study related to the present work[35], however, we concluded that under both normal and elevated pressure conditions typical of small-molecule analysis, retention shifts may remain minor or even experimentally indistinguishable. This can be attributed to a partial compensation between pressure-induced retention and antagonistic friction-induced thermal effects. While this interpretation is consistent

with several published reports, other studies have described moderate to substantial pressure-dependent retention changes [41].

However, it is noteworthy that many of these investigations employed restriction capillaries connected to the column outlet to intentionally elevate column backpressure, without accounting for the accompanying increase in frictional heating arising from the higher pressure drop. In another study, Nováková and co-workers empirically demonstrated the contribution of frictional heating under such conditions, highlighting the potential limitations of traditional geometrical transfer approaches due to altered axial temperature gradient profiles within the stationary phase [33].

To further examine these observations, we conducted a limited geometrical scaling study analogous to the work of Fallas and co-workers, employing the same test compounds and using a restriction capillary unit [42].

As shown in Fig. 2, application of geometrical scaling principles resulted in consistent selectivity when transitioning from a 100 × 2.1 mm (1.7 µm) column to a 50 × 2.1 mm (1.7 µm) column, and subsequently to a 50 × 2.1 mm (5 µm) column. As expected, the reduction in column length combined with the increase in particle size led to decreased column efficiency, leading to broadened peaks. In contrast, when a restriction capillary was assembled, the system backpressure increased to 978 bar for the 50 × 2.1 mm (5 µm) column, comparable to the 956 bar observed with the 100 × 2.1 mm (1.7 µm) column. Despite the similar pressure levels, distinctly different selectivities were obtained. This observation suggests a substantially altered balance between pressure-related and friction-induced thermal effects within the column. It is important to emphasize that all experiments were performed on the same instrument as in the original study (Acquity Classic), equipped with a preheater unit and a block column heater. Nevertheless, this example clearly demonstrated that variations in instrumental configuration—particularly column dimensions and thermostatting mode—can lead to markedly different manifestations of pressure-, and resulting axial and radial frictional heating effects, ranging from negligible to highly significant. Moreover, different classes of analytes, especially larger or ionic molecules, may respond individually to such thermal and pressure-related changes, necessitating careful interpretation of the underlying cause–effect relationships.

Against this background, we aimed to investigate method transferability across different instrument platforms from a practical perspective. To this end, comprehensive modeling analyses were performed on commonly used systems from multiple vendors, applying it in a real-life case study to assess the extent to which instruments may be considered interchangeable—or non-interchangeable—under varying experimental conditions.

3.2. Design space modeling and comparison

The simplified two-dimensional modeling workflow comprised three consecutive steps, as illustrated in Fig. 3. Following the selection of the two stationary phase formats, the modeling framework was established in accordance with fundamental chromatographic principles, particularly with respect to defining meaningful experimental input ranges.

Based on prior studies, the experimental design included two linear gradient runs for each column format. For the 50 × 2.1 mm column, gradient times of 3 and 9 min (t_{G1} and t_{G2}), whereas for the longer, 100 × 2.1 mm column, gradient times of 5 and 15 min were selected. In all cases, the initial and final organic compositions were fixed at 30–80%B. Additionally, two temperature levels ($T_1 = 20°C$ and $T_2 = 50°C$) were incorporated, resulting in a Design of Experiments (DoE) framework requiring only $2 \times 2 = 4$ input runs per model.

Each separation system (A–D) was evaluated under both non-compensated (default) and compensated V_D conditions. During V_D compensation, the effective V_D was adjusted by introducing an isocratic hold at 30%B, scaled to match the system with the largest V_D (Agilent Infinity 1290 system, $V_D = 0.5$ mL).

In total, $2 \times 2 \times 4 \times 4 = 64$ experimental runs (2 columns, 2 V_D settings, 4 instruments, and 4 modeling experiments) were performed which in turn, enabled comprehensive tracking of separation changes across different UHPLC platforms, with particular emphasis on differences arising from solvent delivery characteristics and column thermostatting configurations. The experiments were conducted in the run order previously proposed by Rácz[20], ensuring appropriate thermal equilibration while optimizing overall analysis time; the complete set of model input experiments was finalized within approximately 14 h.

The resulting run data were subsequently processed and imported into the modeling software for peak tracking and detailed model evaluation.

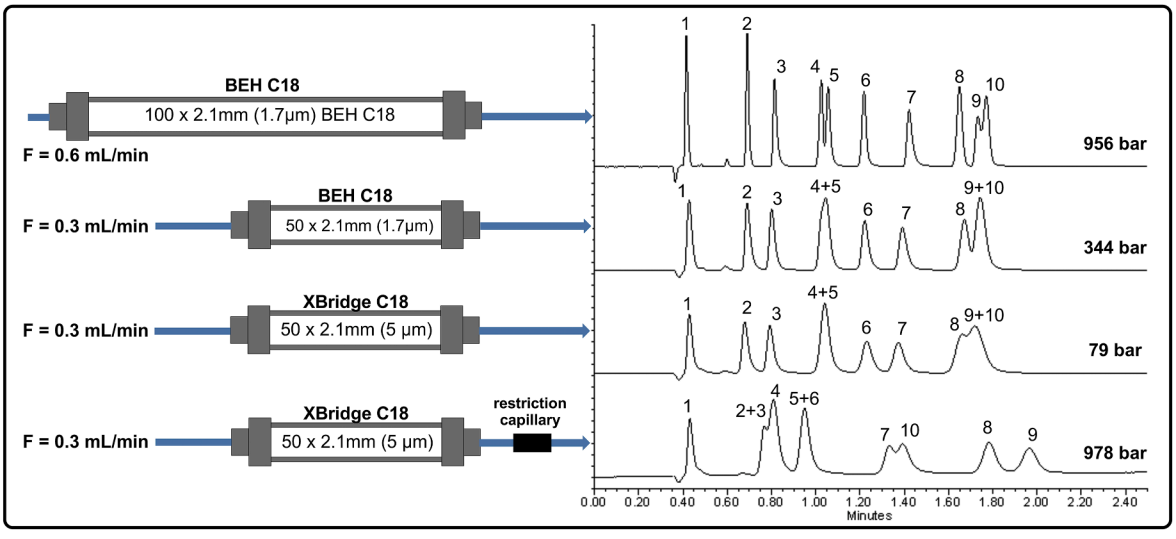


Fig. 2. Experimental reproduction of a literature example using geometrically scaled columns operated with and without a restriction capillary. Chromatograms show a 10-compound mixture of ionizable analytes at different average column pressures, obtained either without or with a 10 cm × 25 µm I.D. restriction capillary. Peaks: 1, thiourea; 2, 2-methylbenzylamine; 3, pyridine; 4, 2,6- lutidine; 5, 2-picoline; 6, 2,4-lutidine; 7, 3-picoline; 8, aniline; 9, benzyl alcohol; 10, 3,4-lutidine. Eluent: acetonitrile–0.025 M potassium phosphate adjusted to pH 5.8 (15:85, v/v), T = 30°C.

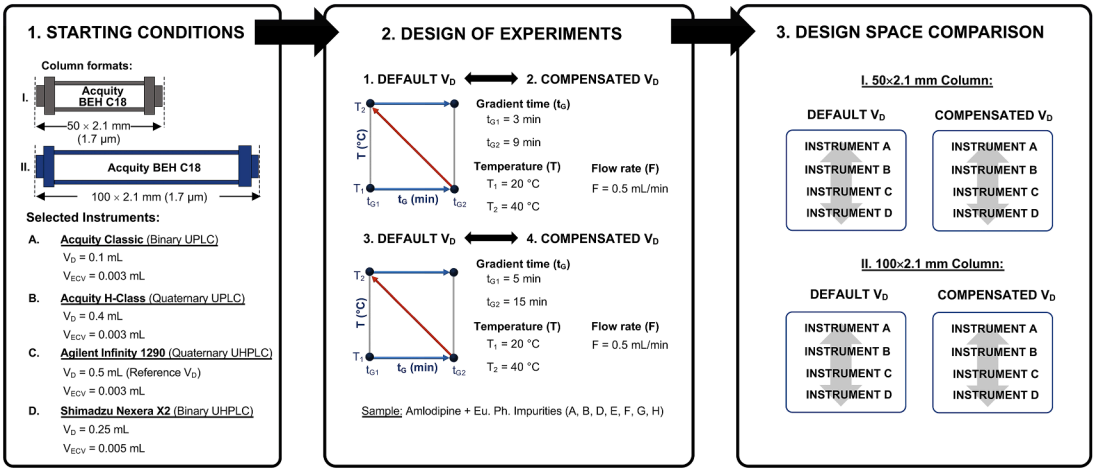


Fig. 3. Applied systematic development scheme for building up and comparing individual multidimensional models of the selected instruments based on their default and compensated dwell volumes.

4. Results and discussion

4.1. Traditional V_D-compensation strategies

As earlier mentioned, when transferring methods between systems, a common practice is to adjust the duration of an initial isocratic segment allowing V_D differences to be readily compensated. USP-NF <621> further defines that "*Monographs preferably include an isocratic step before the start of the gradient program so that an adaptation can be made to the gradient time points to take account of differences in dwell volume between the system used for analytical procedure development and that actually used. It is the user's responsibility to adapt the length of the isocratic step to the analytical equipment used.*" [3]

Indeed, this methodology has been successfully leveraged into practice in other use cases [16,35]. In the present study (Fig. 4) under the selected conditions (t_G = 9 min, T = 20°C), operating the instruments with uncompensated V_Ds led to shifts in retention and peak selectivities. Notably, the Infinity 1290 showed coelution of the critical impurities G and B, which was similarly observed on the quaternary H-Class system. In contrast, the two binary systems (Classic and Nexera X2) produced comparable selectivities; however, the Nexera X2 exhibited a retention delay exceeding initial expectations. The V_D-difference between these two systems was 0.15 mL, which, at a flow rate of 0.5 mL/min, corresponds to only 0.3 min. Nevertheless, a retention shift of 0.6–0.8 min was observed.

The differences became even more pronounced when V_D compensation to 0.5 mL was experimentally implemented. Under these conditions, all systems except one produced comparable chromatographic results, although impurities G and B began to separate visibly on the H-Class system. However, the Nexera X2 showed a significant deviation, largely maintaining the original selectivity pattern observed prior to V_D compensation. This finding indicates instrument-specific behavior that cannot be explained by V_D differences alone. The different column-oven design of the Nexera X2 system may contribute to this behavior; however, the present experimental design does not allow the individual effects of column thermal management, solvent delivery, mixing accuracy, compressibility compensation, and pressure-related thermal phenomena to be independently deconvoluted. Therefore, the observed deviation is interpreted here as a system-specific transferability effect rather than as direct evidence of a single underlying mechanism.

An additional practical observation from this figure was the generally consistent peak-shapes across the systems, with the exception of a pronounced peak-tailing observed on the Infinity system, which however, exhibited uniform tailing factors of approximately 1.40 for all

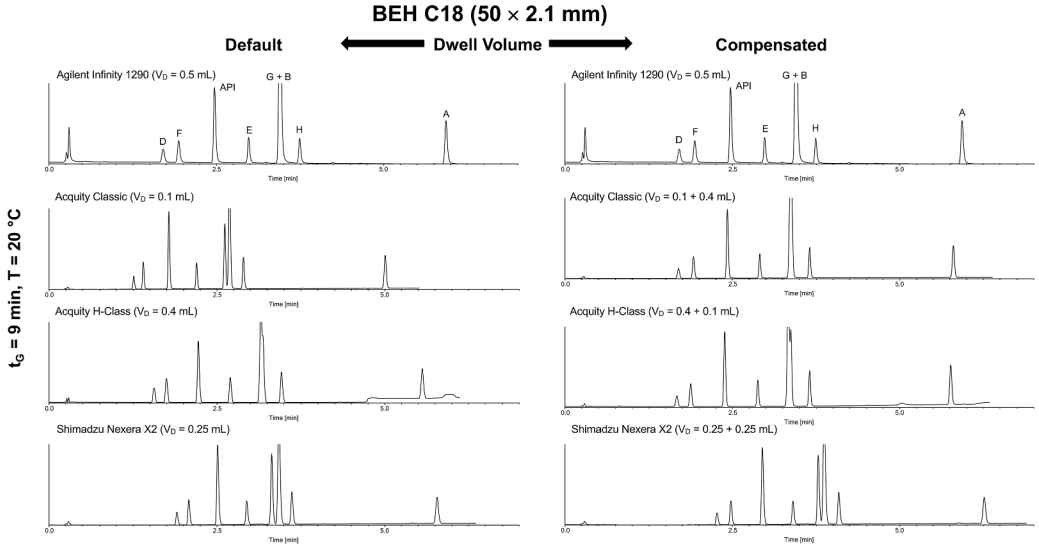


Fig. 4. Comparison of acquired chromatograms at a selected run condition (t_G = 9 min, T = 20°C) with and without dwell volume compensation.

analytes. Under these conditions, there was no indication of detrimental electrostatic interactions, particularly given the symmetrical peak shapes obtained on the other systems. Instead, this pointed to another practical issue related to column hardware compatibility between different instrument brands. Namely, there are several high-pressure fitting standards used in LC-systems today, including Parker, Rheodyne, Swagelok, Waters, and others. Among these, the distance between the tubing tip and the ferrule tip (ferrule setback) may vary, resulting either in insufficient sealing (leading to leakage) or proper sealing but the introduction of additional dead volume, potentially affecting peak shape [11,43].

Since Acquity-series columns were used in our study, they provided native compatibility with corresponding Waters-systems (Classic and H-Class) as well as with the Nexera X2, which was retrofitted with a universal connector (Phenomenex Security Link 25 cm × 100 µm). The Agilent system, however, typically employs a factory-default Swagelok-type connector with a different ferrule setback. In our case, this did not cause solvent leakage but led to uniformly compromised peak shapes, most likely due to the formation of a small extra-column dead volume. Nevertheless, this effect was not critical for the present investigation, as the primary focus was primarily on evaluating selectivity differences across the tested systems.

Finally, it should be noted that universal, tool-free connectors designed for high-pressure operations (up to 1000–1500 bar) are commercially available from various vendors. These high-performance reusable fittings—often utilizing either metal-to-metal or hybrid (metal/PEEK) sealing technologies—help mitigate issues related to ferrule setback variability and ensure zero-dead-volume connections. This further reduces the risk of related performance discrepancies during inter-instrument method transfer.

4.2. Modeling of V_D-compensated systems (50 × 2.1 mm format)

As concluding remarks on the traditional V_D-compensation strategies in the previous section, we observed a certain degree of interchangeability among the tested systems, but also discovered some instrument-specific behavior that could not be fully explained without a broader systematic context.

In contrast, aligned DS models in Fig. 5 delivered detailed insights by capturing separation dynamics of the tested substances within each individual system as well as in their overlaid representation, referred to as the Common Design Space. Within these maps, the blue colored lines indicated two coelutions, one between Imp G–Imp H and the other one between Imp B–Imp G occurring at specific combinations of gradient time and temperature. The trajectories of these coelution curves followed system-specific patterns, visually reflecting slight offsets for each instrument. Notably, the closely overlapping individual heat maps and the converging blue regions within the Common Design Space for the Infinity 1290 and Acquity Classic systems supported the initial observations described in Section 4.1, confirming their practical interchangeability under the investigated conditions. In comparison, more pronounced deviations were observed for the H-Class and Nexera X2 systems, indicating fundamental differences in separation behaviors under the investigated conditions.

Based on this evaluation, operating condition (1–4) at $t_G = 6$ min and T = 45°C was selected from the shared regions of the red-colored Method Operable Design Region (MODR) maps, under which baseline separation ($R_{s,crit} \geq 1.5$) was consistently achieved regardless of the instrument used. This condition, presented in Fig. 6, was subsequently verified experimentally and showed excellent agreement with the modeling results. When comparing the separations obtained on systems 1–3, only minimal differences in retention times were observed, most likely attributable to minor variations in solvent delivery. Similarly, the retention delay previously observed for the forced-air–ventilated Nexera X2 system was also effectively reduced to approximately 0.1–0.2 min relative to the other platforms.

However, this observation should not be interpreted as direct mechanistic evidence that the previously observed Nexera X2 deviation originated solely from column thermostatting. For enthalpy-driven processes, which are characteristic of most chromatographic separations, retention times generally increase at lower temperatures. Nevertheless, the present modeling approach does not allow explicit discrimination between gradient-delivery-related effects, mixing behavior, compressibility management, pressure-induced thermal phenomena, and column-oven-related effects. A more detailed mechanistic separation of these contributions would require targeted experiments, such as temperature-trace measurements, outlet-temperature monitoring, or low-flow control experiments, and is beyond the scope of the present transferability-focused study.

Instead, the results demonstrate that instrument-specific chromatographic behavior can be visualized and managed using a modeling-based Design Space Comparison study. Such behavior may become more pronounced under demanding conditions, but it can also be effectively minimized when operating conditions are selected from a robust common region of the DS. This supports the practical value of the proposed workflow for developing analytical procedures with improved instrument-to-instrument transferability.

4.3. In silico robustness study

In the preceding verification example, all tested systems proved capable of reliably resolving the target analytes under the selected

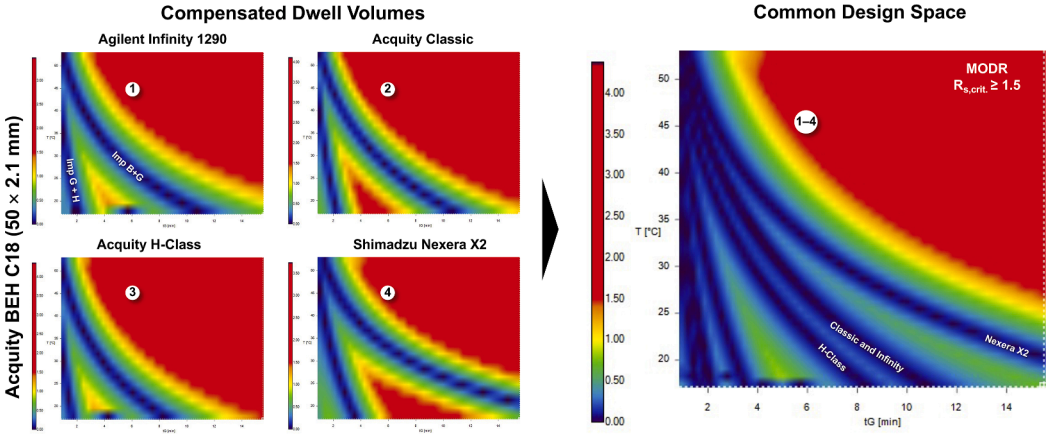


Fig. 5. Individual and combined modeling Design Spaces of the tested UHPLC systems using the 50 × 2.1 mm column. Under the selected condition $t_G = 6$ min, T = 45°C (1–4) all systems were expected to provide comparable baseline separation results.

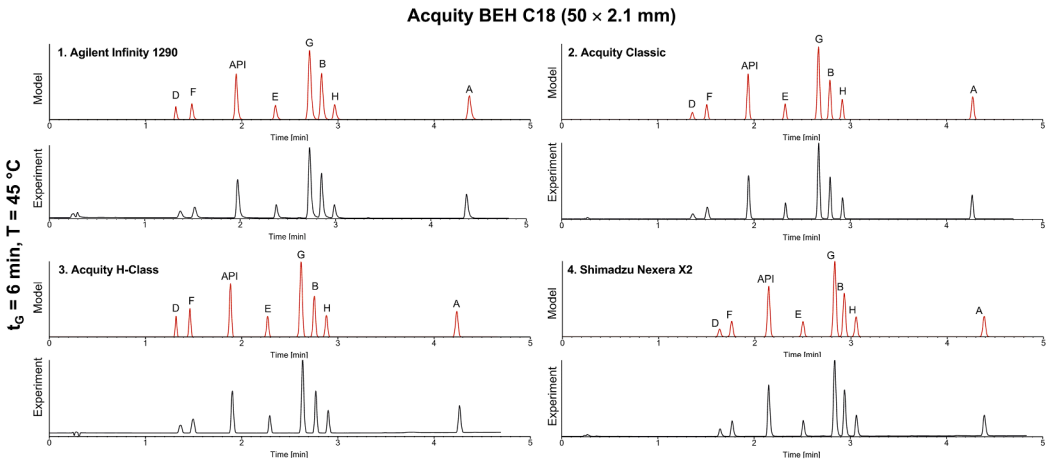


Fig. 6. Experimental verification of a previously selected method (t_G = 6 min, T = 45°C) on the 50 × 2.1 mm column confirming that baseline separation can be achieved on all investigated UHPLC/UPLC platforms when the method is operated within a shared MODR region.

conditions. However, during routine daily application, minor fluctuations in chromatographic parameters—and a subsequent impact on method performance—are to be expected. This variability is addressed through robustness testing, which involves the deliberate variation of analytical parameters. As noted in the ICH Q14 and Q2(R2) guidelines, "*robustness is typically evaluated as part of development prior to the execution of the analytical procedure validation study*" with the outcome directly informing the analytical procedure's control strategy.

A significant advantage of employing chromatography modeling software is its in silico predictive capability, which allows for a comprehensive assessment of method robustness across different chromatographic systems. The validity of this approach has been corroborated by several studies that demonstrate excellent experimental reproducibility between modeled and experimental results [44–46].

Analogously, the impact of potential variations around the nominal setpoints was evaluated using predefined tolerances. The robustness assessment utilized a full-factorial design (3^n) involving five parameters—gradient time, start and end %B, flow rate, and temperature—each evaluated at three levels (+1, 0, −1). V_D variations were excluded from the analysis, as the selected models were generated using compensated volumes (V_D = 0.5 mL). The specific parameter configurations and tolerance levels used for the robustness calculations are summarized in Fig. 7.

As expected, the robustness profiles of the tested systems differed substantially. The frequency distribution histograms for the Acquity Classic and H-Class systems yielded a 100% success rate, while the Infinity 1290 and Nexera X2 systems produced rates of 98.4% and 77.8%, respectively. This indicates that out of the 243 calculated combinations of parameter deviations—including simultaneous changes—the method maintained baseline separation on two instruments but showed certain susceptibility to failure on the two others. This observation is particularly relevant in the context of method transfer. A nominal operating point may appear acceptable on a target instrument when evaluated only under the exact setpoint conditions, yet still be unsuitable from a lifecycle perspective if it lies close to the edge of the instrument-specific MODR. In such a case, routine fluctuations in temperature, flow rate, gradient formation, or mobile-phase composition may shift the separation outside the acceptable region and lead to loss of critical resolution. Therefore, transferability should not be assessed solely by verifying whether the nominal setpoint provides baseline separation, but also by

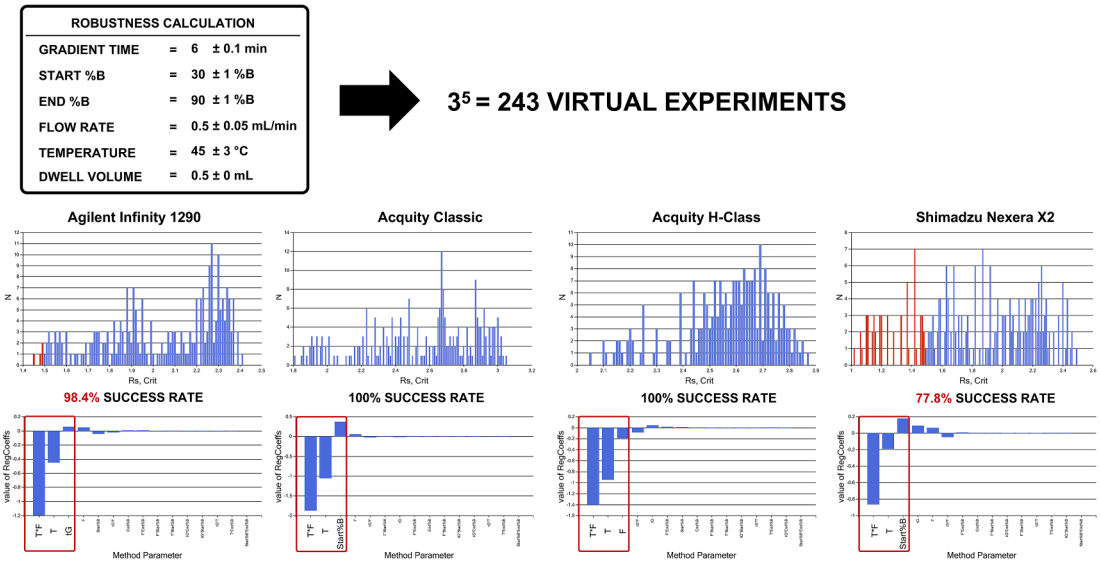


Fig. 7. In silico robustness assessment across multiple HPLC systems. While two systems demonstrate the required separation performance under the current setpoint and tolerance configurations, the remaining systems require more stringent controls during method transfer. In such cases, preventive strategies—including minor adjustments to the original method or the tightening of tolerance limits—ensure consistent separation performance across all platforms.

evaluating the robustness margin around that setpoint on each target system.

Furthermore, the modeling tool ranked the influential parameters (regression coefficients) based on their contribution to critical resolution changes. This highlighted a combined influence of temperature, flow rate, and start %B, though the magnitude of these effects varied across different instruments under identical experimental conditions.

To address these robustness discrepancies, two preventive strategies were evaluated. First, tighter tolerances can be implemented for systems prone to failure; for instance, reducing the temperature tolerance for the Infinity 1290 system to T = 45 ± 2°C resulted in a 100% success rate (**Annex 1**). In contrast, the Nexera X2 system was already approaching its Edge of Failure (EoF), therefore slight adjustment of the initial setpoints was more effective than implementing tighter tolerance controls. Adjusting the column oven to T = 48 ± 3°C and start %B to 32 ± 1 while maintaining all other parameters, achieved a 100% success rate (**Annex 2**).

The third, and from a transferability perspective most generally applicable, strategy involved selecting a common condition located deeper within the shared MODR shown in Fig. 5. This approach directly addresses the risk that a nominally acceptable transferred condition may be positioned near the edge of the MODR on one of the target instruments. Increasing the gradient time to 7.5 min, while keeping all other parameters and tolerances unchanged, resulted in a consistent 100% robustness success rate across all selected instruments **(Annex 3**). However, as separations may behave differently across these systems, the overall resolution values and the identified critical separation parameters (CSPs) varied slightly. By understanding these nuances, suitable control strategies can be established tailored to the specific instrument in use.

Ultimately, any of the calculated robustness scenarios (243 virtual runs per instrument) can be selected for subsequent experimental confirmation. More importantly, the instrument-specific DSs and robustness fingerprints reveal not only whether a nominal method condition is transferable, but also how much robustness margin remains around that condition on each system. This distinction is critical during method transfer, because a condition that is acceptable at the nominal setpoint may still be located close to the edge of the MODR on another instrument and may therefore fail under routine parameter fluctuations. In this sense, DoE-based chromatographic modeling tools such as DryLab provide a substantial advantage over single-point transfer verification, as they allow transferable and robust operating regions to be identified before routine implementation [16,47–49].

4.4. Modeling of V_D-compensated systems (100 × 2.1 mm format)

To broaden the scope of this investigation, the modeling characterization was repeated using a longer 100 × 2.1 mm column packed with the same stationary phase material (1.7 µm BEH C18). The increased column length resulted in substantially higher backpressures, reaching approximately 860–960 bar at 20°C at the gradient start (30 %B), depending on the instrument (Nexera X2 showing the lowest and H-Class the highest values). This enabled closer assessment of more pronounced viscous friction and temperature-related effects. At this stage, smaller (1.0 mm) or larger (3.0 or 4.6 mm) internal diameters, as well as alternative particle sizes, were not considered, as modern UHPLC systems are most commonly operated with highly efficient 50 or 100 × 2.1 mm columns packed with sub-2 µm particles.

Nevertheless, any modification of column hardware inherently alters column backpressure profiles and may shift the established balance between pressure-related effects and friction-induced thermal gradients within the column. Such changes may manifest differently across instrument platforms due to variations in both solvent delivery and column thermostatting mode.

In line with this and the beneficial use of a longer column, Fig. 8 shows a substantial expansion of baseline-separation regions, reflected by the enlarged red areas in the heat maps. Although it was possible to define a well-performing, interchangeable method across all instruments at elevated temperatures (upper red region of the maps), we intentionally aimed to identify conditions under which the Nexera X2 could also serve as a viable alternative at lower temperatures. As shown, a universally shared separation condition across all four tested systems within a reasonable analysis time was not achievable (see bottom-left red region of the heat maps). Therefore, a working condition of t_G = 10 min and T = 20°C was selected. Under these conditions, the chromatograms exhibited greater differences between instruments when compared with the previously selected shorter column experiments. While the elution order and baseline separation were generally preserved, noticeable retention shifts and the formation of different critical peak pairs were observed among the Infinity 1290, Acquity Classic, and Nexera X2 systems. Clearly, under this selected condition, the H-Class system did not provide baseline separation. This, however, does not indicate a fundamental limitation of the particular system itself; for example, at t_G = 8 min and T = 20°C, suitable separation conditions were identified with the other systems, though not with the Nexera X2. Further inspection of the heat maps and modeled chromatograms revealed a higher degree of similarity between the two quaternary systems (Infinity 1290 and H-Class) and between the two binary systems (Acquity Classic and Nexera X2).

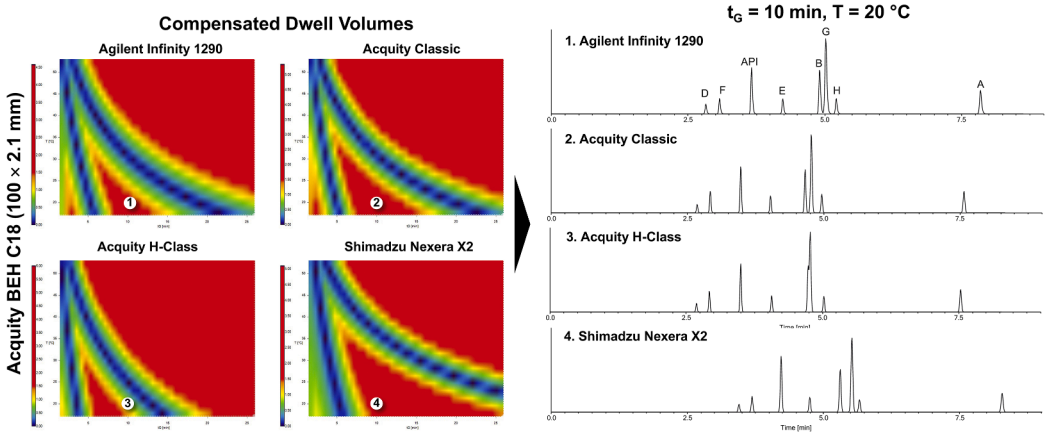


Fig. 8. Individual Design Spaces of the modeled UHPLC systems with dwell volume compensation using the 100 × 2.1 mm column. Selected run condition (1–4) was t_G = 10 min, T = 20°C, the corresponding modeling chromatograms are displayed on the right.

In summary, these findings indicate that method transferability may become more challenging under demanding UHPLC conditions, particularly when operating at elevated backpressure and below ambient temperature. Under such conditions, pressure-related viscous heat generation may complicate thermal control, while pressure-dependent compressibility effects may influence solvent-delivery and gradient-formation consistency. In addition, differences in mixing behavior, column thermostatting, and instrument-specific fluidic design may further contribute to system-dependent retention and selectivity changes [9,32]. Therefore, such effects should be interpreted as the combined outcome of several interrelated instrumental factors rather than as the consequence of backpressure alone. In these development scenarios, DS modeling becomes especially valuable because it allows instrument-specific behavior to be visualized, compared, and managed through rational method adjustment.

4.5. Modeling on instruments with default V_Ds (100 × 2.1 mm format)

Finally, to further demonstrate the validity and practical utility of the presented modeling approach, we conducted a comparable study on the same, 100 mm-long stationary phase, but this time without implementing V_D-compensation between instruments, thereby moving beyond the regulatory suggestions. The resulting heat maps in Fig. 9 exhibited minor shifts relative to those in Fig. 8, except for the Infinity 1290 system, where the V_D remained unchanged at 0.5 mL.

By selecting a working condition at elevated temperature (t_G = 10 min, T = 45°C), a somewhat unexpected similarity in selectivity and overall retention window was observed between the Infinity 1290 and Nexera X2 systems, and to a lesser extent with the H-Class. This apparent convergence may result from the combined effects previously discussed. In marked contrast, the Acquity Classic system—characterized by the lowest V_D—exhibited a comparable selectivity profile but with substantially earlier peak elution.

Taken together, this example further highlights the dynamic and interdependent nature of chromatographic separations. Rather than relying solely on single-parameter V_D- compensation strategies, systematic DS analysis enabled the exploration of alternative compensation approaches. A comparable strategy was also described by Nováková [33], who mitigated increasing viscous friction effects by lowering column temperature. Based on our findings, differences related to gradient delay, solvent delivery, and pressure-induced thermal effects can likewise be empirically managed through multidimensional model analysis.

5. Conclusion

Building on our previous investigations, this study evaluated the feasibility of establishing a more efficient strategy for managing instrument-to-instrument transferability of gradient UHPLC methods. Although conventional approaches such as geometrical scaling and V_D compensation provide practical means for method transfer, they do not fully account for additional differences arising from instrument-specific characteristics, including variations in solvent-delivery behavior and thermally induced effects within the column.

To our knowledge, this is the first study to utilize a systematic modeling framework to elucidate dynamic variations across chromatographic platforms from various vendors commonly found in analytical laboratories. By performing a series of four targeted experiments per system, we constructed individual two-dimensional DSs for four representative platforms—Agilent Infinity 1290, Waters Acquity Classic, Waters H-Class, and Shimadzu Nexera X2. This approach allowed us to characterize and compare the combined effects of backpressure, viscous friction, and gradient delay, alongside hardware-specific solutions. Our results demonstrate that while these systems can behave interchangeably under certain conditions, instrument-specific effects become significantly more pronounced under demanding UHPLC conditions—particularly at elevated backpressures and below ambient temperatures.

Furthermore, we successfully demonstrated that in silico modeling is a powerful tool for assessing and mitigating robustness-related risks associated with innate instrument-to-instrument variabilities. By individually quantifying robustness across multiple platforms, we have shown that system-specific performance discrepancies can be proactively managed through targeted setpoint adjustments or refined tolerance limits.

Ultimately, this framework moves beyond traditional trial-and-error method transfer, providing the transparency needed to create more rugged and globally transferable analytical procedures.

CRediT authorship contribution statement

Arnold Zöldhegyi: Writing – original draft, Methodology, Investigation. **Krisztián Horváth:** Writing – review & editing. **Imre Molnár:** Writing – review & editing. **Róbert Kormány:** Writing – original draft, Methodology, Investigation, Conceptualization.

Declaration of competing interest

The authors declare that they have no known competing financial interests or personal relationships that could have appeared to influence the work reported in this paper.

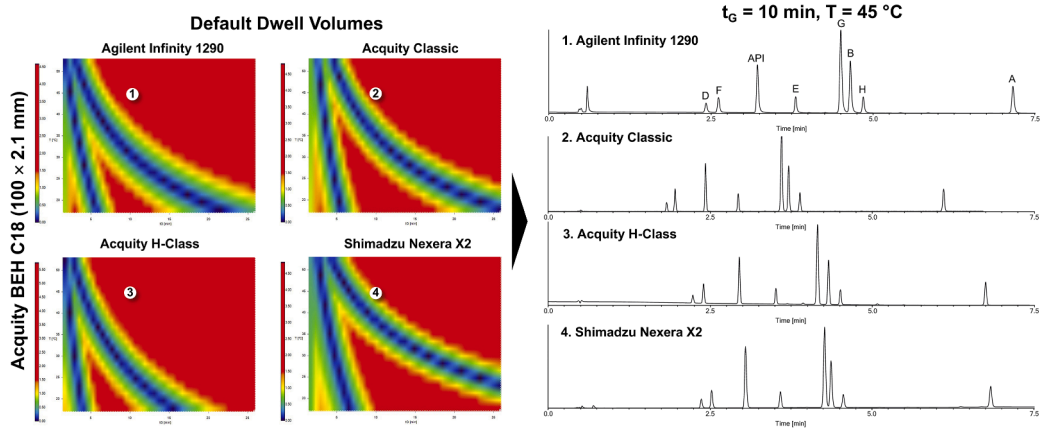
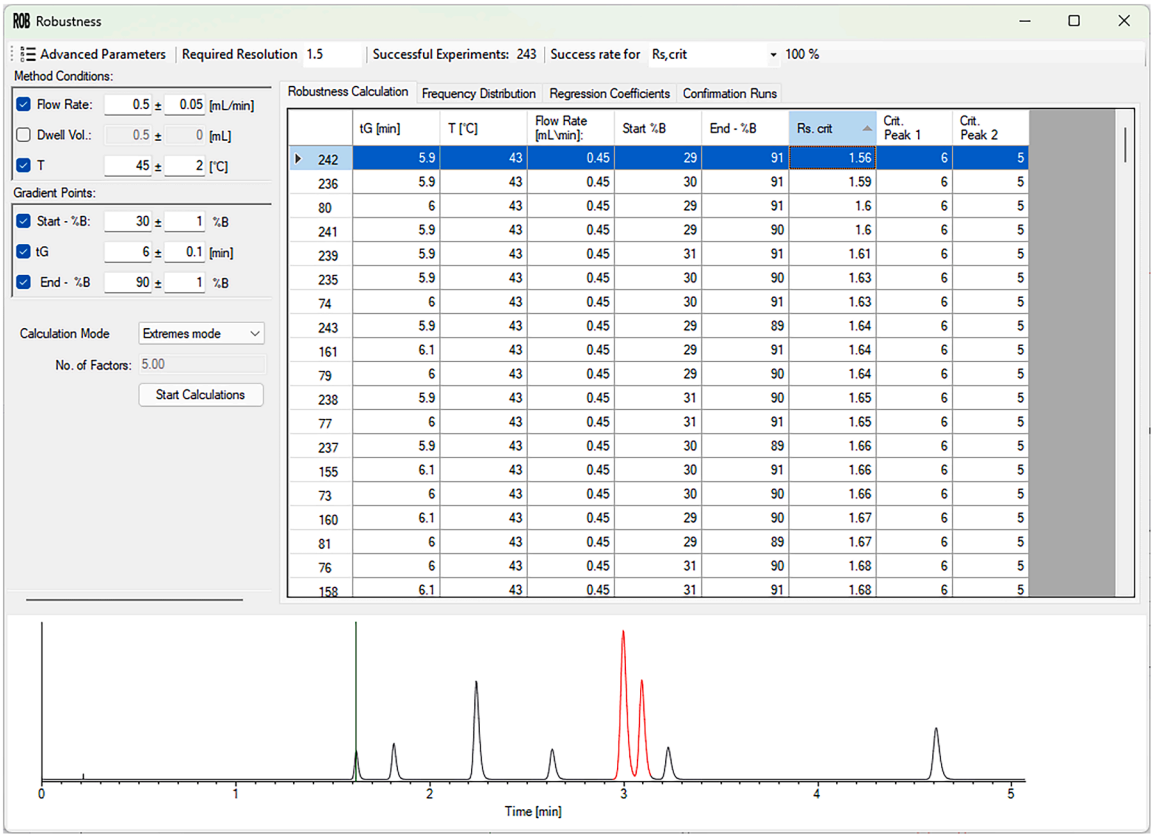


Fig. 9. Individual Design Spaces of the modeled UHPLC systems without dwell volume compensation using the 100 × 2.1 mm column. The selected run condition (1–4) was t_G = 10 min, T = 45°C, the corresponding acquired chromatograms are displayed on the right.

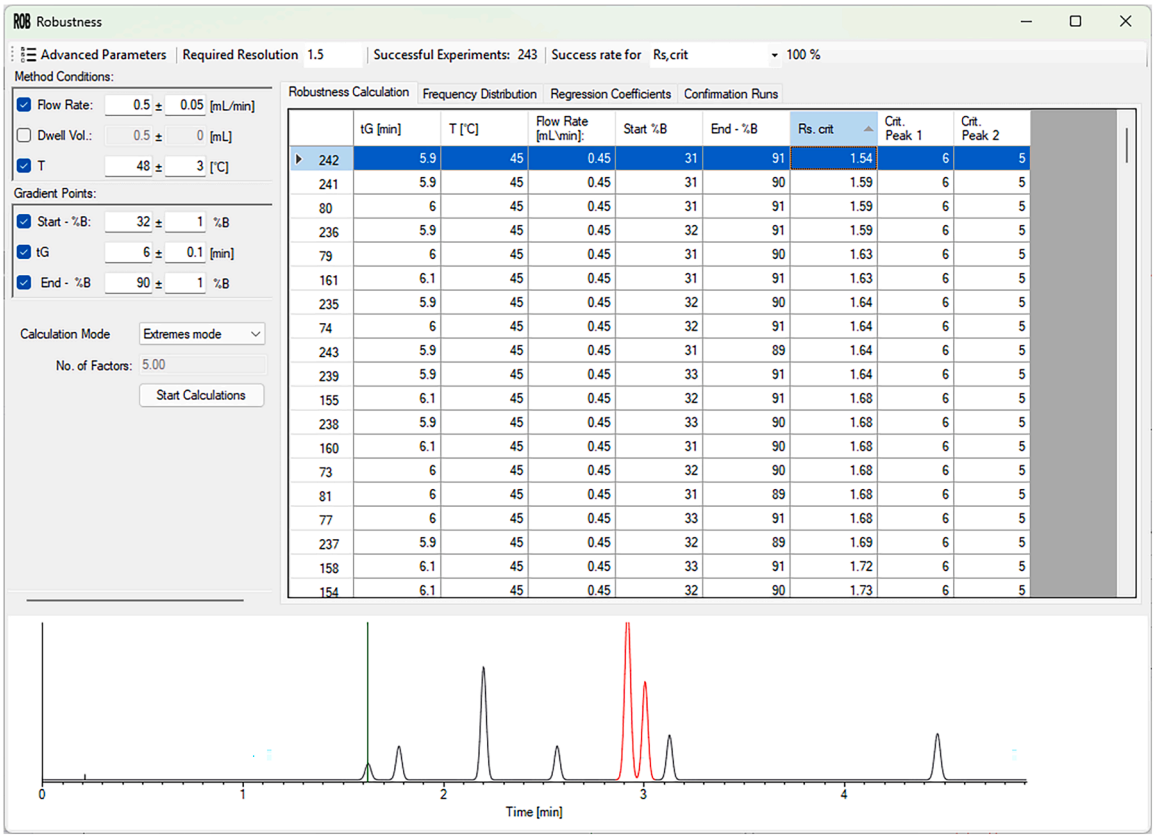
Annex 1. Robustness modeling study on the Agilent Infinity 1290 system. The robustness study comprised $3^5 = 243$ virtual calculations; initially, 98.4% of the results met the success criteria. Tightening the temperature limits from ± 3°C to ± 2°C increased the success rate to 100%, indicating a fully robust separation within the refined limits. In the calculation table, results are sorted in ascending order of critical resolution ($R_{s,crit.}$). The lower panel illustrates the modeled chromatogram for the worst-performing experiment (the "worst-case scenario")



	tG [min]	T [°C]	Flow Rate [mL\min]:	Start %B	End - %B	Rs, crit	Crit. Peak 1	Crit. Peak 2
242	5.9	43	0.45	29	91	1.56	6	5
236	5.9	43	0.45	30	91	1.59	6	5
80	6	43	0.45	29	91	1.6	6	5
241	5.9	43	0.45	29	90	1.6	6	5
239	5.9	43	0.45	31	91	1.61	6	5
235	5.9	43	0.45	30	90	1.63	6	5
74	6	43	0.45	30	91	1.63	6	5
243	5.9	43	0.45	29	89	1.64	6	5
161	6.1	43	0.45	29	91	1.64	6	5
79	6	43	0.45	29	90	1.64	6	5
238	5.9	43	0.45	31	90	1.65	6	5
77	6	43	0.45	31	91	1.65	6	5
237	5.9	43	0.45	30	89	1.66	6	5
155	6.1	43	0.45	30	91	1.66	6	5
73	6	43	0.45	30	90	1.66	6	5
160	6.1	43	0.45	29	90	1.67	6	5
81	6	43	0.45	29	89	1.67	6	5
76	6	43	0.45	31	90	1.68	6	5
158	6.1	43	0.45	31	91	1.68	6	5

Selected conditions are $t_G = 6 \pm 0.1$ min, T = 45 ± 3°C, start %B = 30 ± 1 and end %B = 90 ± 1 and F = 0.5 ± 0.05. Column: Acquity BEH C18 50 × 2.1 mm (1.7 μm), $V_D = 0.5$ mL.

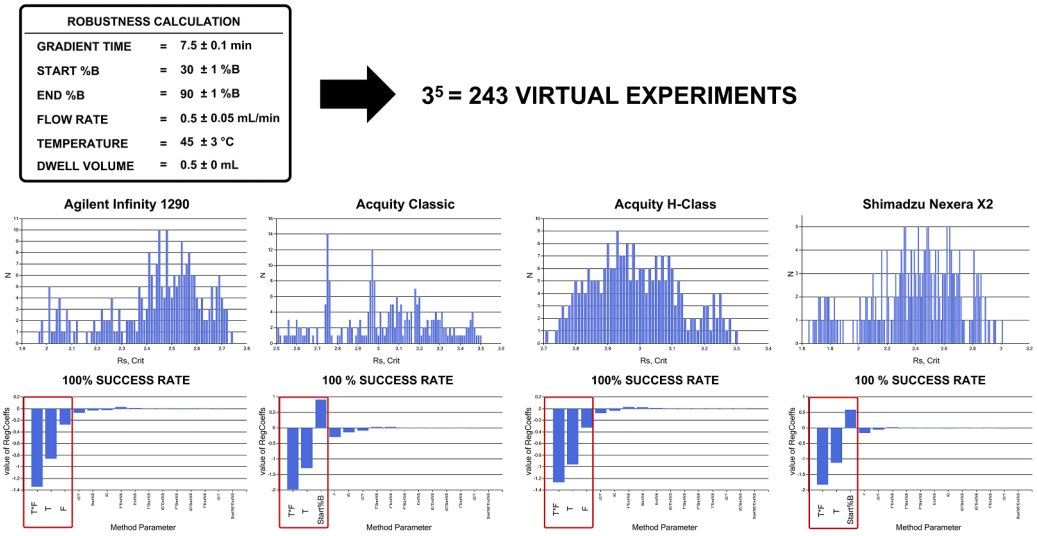
Annex 2. Robustness modeling study on the Shimadzu Nexera X2 system. The robustness study comprised $3^5 = 243$ virtual calculations; initially, 77.8% of the results met the success criteria. By refining the initial setpoints to T = 48 ± 3°C and start %B to 32 ± 1, success rate was increased to 100%, ensuring fully robust separation within the new specification. In the calculation table, results are sorted in ascending order of critical resolution ($R_{s,crit.}$). The lower panel illustrates the modeled chromatogram for the worst-performing experiment (the "worst-case scenario")



	tG [min]	T [°C]	Flow Rate [mL\min]:	Start %B	End - %B	Rs, crit	Crit. Peak 1	Crit. Peak 2
242	5.9	45	0.45	31	91	1.54	6	5
241	5.9	45	0.45	31	90	1.59	6	5
80	6	45	0.45	31	91	1.59	6	5
236	5.9	45	0.45	32	91	1.59	6	5
79	6	45	0.45	31	90	1.63	6	5
161	6.1	45	0.45	31	91	1.63	6	5
235	5.9	45	0.45	32	90	1.64	6	5
74	6	45	0.45	32	91	1.64	6	5
243	5.9	45	0.45	31	89	1.64	6	5
239	5.9	45	0.45	33	91	1.64	6	5
155	6.1	45	0.45	32	91	1.68	6	5
238	5.9	45	0.45	33	90	1.68	6	5
160	6.1	45	0.45	31	90	1.68	6	5
73	6	45	0.45	32	90	1.68	6	5
81	6	45	0.45	31	89	1.68	6	5
77	6	45	0.45	33	91	1.68	6	5
237	5.9	45	0.45	32	89	1.69	6	5
158	6.1	45	0.45	33	91	1.72	6	5
154	6.1	45	0.45	32	90	1.73	6	5

Selected conditions are $t_G = 6 \pm 0.1$ min, T = 48 ± 3°C, start %B = 32 ± 1 and end %B = 90 ± 1 and F = 0.5 ± 0.05. Column: Acquity BEH C18 50 × 2.1 mm (1.7 μm), $V_D = 0.5$ mL.

Annex 3. In silico robustness assessment across multiple HPLC systems. Under the redefined experimental conditions and maintained tolerance settings, the model confirms that all systems provide robust separation. The analysis also quantifies the contributions of critical separation parameters, enabling the development of meaningful analytical control strategies for ensuring a robust method lifecycle



Selected conditions are $t_G = 7.5 \pm 0.1$ min, T = 45 ± 3°C, start %B = 30 ± 1 and end %B = 90 ± 1 and F = 0.5 ± 0.05. Column: Acquity BEH C18 50 × 2.1 mm (1.7 μm), $V_D = 0.5$ mL.

Data availability

Data will be made available on request.

Bibliography

[1] International council for harmonisation of technical requirements for pharmaceuticals for human use. Analytical procedure development Q14. https://database.ich.org/sites/default/files/ICH_Q14_Guideline_2023_1130_ErrorCorrection_2025.pdf, 2023.

[2] International council for harmonisation of technical requirements for pharmaceuticals for human use. Validation of analytical procedures Q2(R2). https://database.ich.org/sites/default/files/ICH_Q2%28R2%29_Guideline_2023_1130.pdf, 2023.

[3] United States Pharmacopoeia, USP <621>chromatography. https://doi.usp.org/USPNF/USPNF_M99380_70101_01.html, 2022.

[4] L.S. Ettre, Csaba Horváth and the development of the first modern high performance liquid chromatograph | LCGC international. https://www.chromatographyonline.com/view/csaba-horv-th-and-development-first-modern-high-performance-liquid-chromatograph, 2005.

[5] Milestones in the development of liquid chromatography, Liquid Chromatography, Elsevier, 2023, pp. 1–15, https://doi.org/10.1016/B978-0-323-99968-7.00001-1.

[6] HPLC instrumentation in pharmaceutical analysis: status, advances, and trends, in: Separation Science and Technology, 6, Academic Press, 2005, pp. 47–75, https://doi.org/10.1016/S0149-6395(05)80047-9.

[7] C.S. Raska, T.S. Bennett, S.A. Goodberlet, Risk-based analytical method transfer: application to large multi-product transfers, Anal. Chem. 82 (14) (2010) 5932–5936, https://doi.org/10.1021/ac1008892.

[8] Method validation, Introduction to Modern Liquid Chromatography, John Wiley & Sons, Ltd, 2009, pp. 531–567, https://doi.org/10.1002/9780470508183.ch12.

[9] S. Fekete, I. Kohler, S. Rudaz, D. Guillarme, Importance of instrumentation for fast liquid chromatography in pharmaceutical analysis, J. Pharm. Biomed. Anal. 87 (2014) 105–119, https://doi.org/10.1016/j.jpba.2013.03.012.

[10] Moldoveanu, S.; David, V. Overview of HPLC instrumentation and its use; 2022; pp 21–61. https://doi.org/10.1016/B978-0-323-91177-1.00015-6.

[11] L.R. Snyder, J.J. Kirkland, J.W. Dolan, Introduction to Modern Liquid Chromatography, Equipment. In, John Wiley & Sons, Ltd, 2009, pp. 87–145, https://doi.org/10.1002/9780470508183.ch3.

[12] W.R. LaCourse, M.E. LaCourse, General instrumentation in HPLC. Liquid Chromatography, Elsevier, 2023, pp. 61–73, https://doi.org/10.1016/B978-0-323-99968-7.00009-6.

[13] A.P. Schellinger, P.W. Carr, A practical approach to transferring linear gradient elution methods, J. Chromatogr. A 1077 (2) (2005) 110–119, https://doi.org/10.1016/j.chroma.2005.04.088.

[14] D. Guillarme, D.T.T. Nguyen, S. Rudaz, J.-L. Veuthey, Method transfer for fast liquid chromatography in pharmaceutical analysis: application to short columns packed with small particle. Part II: gradient experiments, Eur. J. Pharm. Biopharm. 68 (2) (2008) 430–440, https://doi.org/10.1016/j.ejpb.2007.06.018.

[15] M. Metzlaff, Agilent 1260 Infinity II Prime LC with ISET. https://www.agilent.com/cs/library/applications/5991-8786EN_InfinityII_Application.pdf?srsltid=AfmBOoqg2-EzlcAO9_2aBVVdaQesg4P8olQLysPhC8UiPejmDp-khvHg, 2024.

[16] D. Enesei, I. Kapui, S. Fekete, R. Kormány, Updating the European pharmacopoeia impurity profiling method for terazosin and suggesting alternative columns, J. Pharm. Biomed. Anal. 187 (2020) 113371, https://doi.org/10.1016/j.jpba.2020.113371.

[17] U.D. Neue, Column design. HPLC Columns: Theory, Technology, and Practice, Wiley VCH, New York, NY, 1997, pp. 41–80.

[18] R. Kormány, Optimized UHPLC–Derivatization method for low-level nitrite detection in pharmaceutical excipients (In Print), J. Pharm. Biomed. Anal. 276 (2026) 117472.

[19] R. Kormány, I. Molnár, J. Fekete, D. Guillarme, S. Fekete, Robust UHPLC separation method development for multi-API product containing amlodipine and bisoprolol: the impact of column selection, Chromatographia 77 (17) (2014) 1119–1127, https://doi.org/10.1007/s10337-014-2633-9.

[20] N. Rácz, R. Kormány, J. Fekete, I. Molnár, Establishing column batch repeatability according to quality by design (QbD) principles using modeling software, J. Pharm. Biomed. Anal. 108 (2015) 1–10, https://doi.org/10.1016/j.jpba.2015.01.037.

[21] U.D. Neue, Reversed-phase chromatography. HPLC columns: Theory, Technology, and Practice, Wiley VCH, New York, NY, 1997, pp. 183–216.

[22] L.R. Snyder, J.J. Kirkland, J.W. Dolan, Basic concepts and the control of separation. Introduction to Modern Liquid Chromatography, John Wiley & Sons, Ltd, 2009, pp. 19–86, https://doi.org/10.1002/9780470508183.ch2.

[23] S. Heinisch, J.-L. Rocca, Sense and nonsense of high-temperature liquid chromatography, J. Chromatogr. A 1216 (4) (2009) 642–658, https://doi.org/10.1016/j.chroma.2008.11.079.

[24] S. Fekete, S. Rudaz, J. Fekete, D. Guillarme, Analysis of recombinant monoclonal antibodies by RPLC: toward a generic method development approach, J. Pharm. Biomed. Anal. 70 (2012) 158–168, https://doi.org/10.1016/j.jpba.2012.06.021.

[25] B. Soós, K. Horváth, R. Kormány, The dynamic balances in HPLC: an unconventional application of temperature to optimize ionizable solute separations, J. Chromatogr. A 1760 (2025) 466268, https://doi.org/10.1016/j.chroma.2025.466268.

[26] European Pharmacopoeia 10.8, Spectinomycin Dihydrochloride Pentahydrate (2022), 07/2022:1152.

[27] H. Poppe, J.C. Kraak, J.F.K. Huber, J.H.M van den Berg, Temperature gradients in HPLC columns due to viscous heat dissipation, Chromatographia 14 (9) (1981) 515–523, https://doi.org/10.1007/BF02265631.
[28] T. Welsch, M. Schmid, J. Kutter, A. Kálman, Temperature of the eluent: a neglected tool in high-performance liquid chromatography? J. Chromatogr. A 728 (1–2) (1996) 299–306, https://doi.org/10.1016/0021-9673(95)00876-4.
[29] M. Heidorn, S. Fabel, F. Steiner, Thermostatting in UHPLC: forced air mode, still air mode, and method transfer. https://documents.thermofisher.com/TFS-Assets/CMD/posters/PN-71314-ISC2014-UHPLC-Thermostatting-PN71314-EN.pdf, 2016.
[30] I. Halász, R. Endele, J. Asshauer, Ultimate limits in high-pressure liquid chromatography, J. Chromatogr. A 112 (1975) 37–60, https://doi.org/10.1016/S0021-9673(00)99941-2.
[31] C. Horváth, H.-J. Lin, Band spreading in liquid chromatography: general plate height equation and a method for the evaluation of the individual plate height contributions, J. Chromatogr. A 149 (1978) 43–70, https://doi.org/10.1016/S0021-9673(00)80978-4.
[32] F. Gritti, G. Guiochon, Effects of the thermal heterogeneity of the column on chromatographic results, J. Chromatogr. A 1131 (1) (2006) 151–165, https://doi.org/10.1016/j.chroma.2006.07.051.
[33] L. Nováková, J.L. Veuthey, D. Guillarme, Practical method transfer from high performance liquid chromatography to ultra-high performance liquid chromatography: the importance of frictional heating, J. Chromatogr. A 1218 (44) (2011) 7971–7981, https://doi.org/10.1016/j.chroma.2011.08.096.
[34] O. Peterka, A. Langová, R. Jirásko, M. Holčapek, Bioinert UHPLC system improves sensitivity and peak shapes for ionic metabolites, J. Chromatogr. A 1740 (2025) 465588, https://doi.org/10.1016/j.chroma.2024.465588.
[35] R. Kormány, J. Fekete, D. Guillarme, S. Fekete, Reliability of computer-assisted method transfer between several column dimensions packed with 1.3–5 μm core–shell particles and between various instruments, J. Pharm. Biomed. Anal. 94 (2014) 188–195, https://doi.org/10.1016/j.jpba.2014.01.037.
[36] A. Zöldhegyi, K. Horváth, R. Kormány, Revisiting column selectivity choices in ultra-high performance liquid chromatography–using multidimensional analytical design spaces to identify column equivalency, J. Chromatogr. A 1719 (2024) 464738, https://doi.org/10.1016/j.chroma.2024.464738.
[37] B. Duivelshof, A. Zöldhegyi, D. Guillarme, M. Lauber, S. Fekete, Expediting the chromatographic analysis of COVID-19 antibody therapeutics with ultra-short columns, retention modeling and automated method development, J. Pharm. Biomed. Anal. 221 (2022) 115039, https://doi.org/10.1016/j.jpba.2022.115039.
[38] R. Kormány, B. Soós, K. Horváth, Updating the European pharmacopoeia impurity profiling method for Cetirizine and suggesting alternative column, using design space comparison, J. Pharm. Biomed. Anal. 237 (2024) 115776, https://doi.org/10.1016/j.jpba.2023.115776.
[39] A. Zöldhegyi, B. Soós, K. Horváth, I. Molnár, R. Kormány, Extended multidimensional design space studies: comparing volatile and non-volatile buffer systems in UPLC, J. Chromatogr. A 1751 (2025) 465951, https://doi.org/10.1016/j.chroma.2025.465951.
[40] S. Fekete, M. Fogwill, M.A. Lauber, Pressure-enhanced liquid chromatography, a proof of concept: tuning selectivity with pressure changes and gradients, Anal. Chem. 94 (22) (2022) 7877–7884, https://doi.org/10.1021/acs.analchem.2c00464.
[41] N. Tanaka, T. Yoshimura, M. Araki, Effect of pressure on solute retention in the ionization control mode in reversed-phase liquid chromatography, J. Chromatogr. A 406 (1987) 247–256, https://doi.org/10.1016/S0021-9673(00)94033-0.
[42] M.M. Fallas, U.D. Neue, M.R. Hadley, D.V. McCalley, Further investigations of the effect of pressure on retention in ultra-high-pressure liquid chromatography, J. Chromatogr. A 1217 (3) (2010) 276–284, https://doi.org/10.1016/j.chroma.2009.11.041.
[43] U.D. Neue, Column maintenance. HPLC Columns: Theory, Technology, and Practice, Wiley VCH, New York, NY, 1997, pp. 342–379.
[44] R. Kormány, J. Fekete, D. Guillarme, S. Fekete, Reliability of simulated robustness testing in fast liquid chromatography, using State-of-the-art column technology, instrumentation and modelling software, J. Pharm. Biomed. Anal. 89 (2014) 67–75, https://doi.org/10.1016/j.jpba.2013.10.029.
[45] A. Zöldhegyi, H.-J. Rieger, I. Molnár, L. Fekhretdinova, Automated UHPLC separation of 10 pharmaceutical compounds using software-modeling, J. Pharm. Biomed. Anal. 156 (2018) 379–388, https://doi.org/10.1016/j.jpba.2018.03.039.
[46] E. Ferencz, A. Zöldhegyi, É.-K. Kelemen, M. Obreja, M. Urkon, E. Sipos, G. Tóth, I. Molnár, Z.-I. Szabó, Analytical quality by design-compliant retention modeling for exploring column interchangeabilities in separating Ezetimibe and its related substances, J. Chromatogr. A 1682 (2022) 463494, https://doi.org/10.1016/j.chroma.2022.463494.
[47] A.H. Schmidt, I. Molnár, Using an innovative quality-by-design approach for development of a stability indicating UHPLC method for ebastine in the API and pharmaceutical formulations, J. Pharm. Biomed. Anal. 78-79 (2013) 65–74, https://doi.org/10.1016/j.jpba.2013.01.032.
[48] A.H. Schmidt, M. Stanic, I. Molnár, In silico robustness testing of a compendial HPLC purity method by using of a multidimensional design space build by chromatography modeling—case study Pramipexole, J. Pharm. Biomed. Anal. 91 (2014) 97–107, https://doi.org/10.1016/j.jpba.2013.12.023.
[49] K. Jayaraman, A.K. Rajendran, G.S. Kumar, H. Bhutani, A methodology employing retention modeling for achieving control space in liquid chromatography method development using quality by design approach, J. Chromatogr. A 1635 (2021) 461658, https://doi.org/10.1016/j.chroma.2020.461658.